Published on: 10 October 2019

DOI: 10.1002/asna.201913673

ORIGINAL ARTICLE

Astronomische Nachrichten

Estimation of the detected background by the future gamma ray transient mission CAMELOT

Jakub Řípa[1,2,3] | Gábor Galgóczi[2] | Norbert Werner[1,4,5] | András Pál[6] | Masanori Ohno[1,2,5,6] | László Mészáros[6] | Tsunefumi Mizuno[7] | Norbert Tarcai[8] | Kento Torigoe[5] | Nagomi Uchida[5] | Yasushi Fukazawa[5] | Hiromitsu Takahashi[5] | Kazuhiro Nakazawa[9] | Naoyoshi Hirade[5] | Kengo Hirose[5] | Syohei Hisadomi[9] | Teruaki Enoto[10] | Hirokazu Odaka[11] | Yuto Ichinohe[12] | Zsolt Frei[2] | László Kiss[6]

[1]MTA-Eötvös University Lendület Hot Universe Research Group, Budapest, Hungary

[2]Institute of Physics, Eötvös University, Budapest, Hungary

[3]Astronomical Institute, Charles University, Prague, Czech Republic

[4]Department of Theoretical Physics and Astrophysics, Faculty of Science, Masaryk University, Brno, Czech Republic

[5]School of Science, Hiroshima University, Higashi-Hiroshima, Japan

[6]Konkoly Observatory of the Hungarian Academy of Sciences, Budapest, Hungary

[7]Hiroshima Astrophysical Science Center, Hiroshima University, Higashi-Hiroshima, Japan

[8]C3S Electronics Development LLC, Budapest, Hungary

[9]Department of Physics, Nagoya University, Nagoya, Japan

[10]The Hakubi Center for Advanced Research and Department of Astronomy, Kyoto University, Kyoto, Japan

[11]Department of Physics, University of Tokyo, Tokyo, Japan

[12]Department of Physics, Rikkyo University, Tokyo, Japan

Correspondence
Jakub Řípa, MTA-Eötvös University Lendület Hot Universe Research Group, Pázmány Péter sétány 1/A, Budapest 1117, Hungary.
Email: jripa@caesar.elte.hu

Abstract

This study presents a background estimation for the CubeSats Applied for MEasuring and LOcalising Transients (CAMELOT), which is a proposed fleet of nanosatellites for the all-sky monitoring and timing-based localization of gamma ray transients with precise localization capability at low Earth orbits. CAMELOT will allow us to observe and precisely localize short gamma ray bursts (GRBs) associated with kilonovae, long GRBs associated with core-collapse massive stars, magnetar outbursts, terrestrial gamma ray flashes, and gamma ray counterparts to gravitational wave sources. A fleet of at least nine 3U CubeSats is proposed to be equipped with large and thin CsI(Tl) scintillators read out by multipixel photon counters (MPPC). A careful study of the radiation environment in space is necessary to optimize the detector casing, estimate the duty cycle due to the crossing of the South Atlantic Anomaly and polar regions, and minimize the effect of the radiation damage of MPPCs.

KEYWORDS

(ISM:) cosmic rays, gamma rays: bursts, instrumentation: detectors, X-rays: diffuse background

Funding information
European Social Fund,
EFOP-3.6.1-16-2016-00023; Hungarian Academy of Sciences, KEP-7/2018,
LP2016-11

1 | INTRODUCTION

CubeSats Applied for MEasuring and LOcalising Transients (CAMELOT) (for details, see Ohno et al. (2018); Pál et al. (2018); Torigoe et al. (2019); Řípa et al. (2018); Werner et al. (2018)) is a future constellation of at least nine 3U CubeSats, which will be primarily monitoring and precisely and rapidly localizing gamma ray bursts (GRBs) (see Klebesadel et al. (1973); Kouveliotou et al. (2012); Vedrenne & Atteia (2009)) over the whole sky. It will allow regular detection of electromagnetic counterparts of gravitation wave sources similar to the breakthrough discovery of the neutron star merger GW170817 (Abbott et al. 2017) associated with a short GRB 170817A (Goldstein et al. 2017). This gamma ray monitoring network will also allow us to observe long GRBs associated with core-collapse massive stars, soft gamma repeaters (SGR) associated with magnetar outbursts (Kouveliotou et al. 1998; Mazets et al. 1979), and terrestrial gamma ray flashes (TGF) produced by thunderstorms (Fishman et al. 1994).

The CAMELOT satellites (see Figure 1) will be equipped with two or four large and thin CsI(Tl) scintillators, $75 \times 150 \times 5$ mm^3 each, read out by multipixel photon counter (MPPC) silicon photomultipliers from Hamamatsu. The scintillators will be enclosed in an Al or carbon fiber-reinforced plastic (CFRP) support structure and will be placed on one or two of the long sides of the satellite, with sensitivity in the range of $\sim 10 - 1,000$ keV.

The intended orbit configurations of the CAMELOT CubeSats are either low earth orbits (LEO) at an altitude of $\sim 500 - 600$ km with inclination of 53° or polar orbits with an inclination of around 97.6°. However, the final decision will depend on the launch opportunities.

Here, we briefly summarize our studies of the impact of the radiation environment in LEO on the CAMELOT satellites carried out to optimize the scintillator casing, estimate the duty cycle due to crossing of the South Atlantic Anomaly (SAA) and polar regions, and design radiation shielding to minimize the effect of the degradation of MPPCs due to the proton fluxes.

2 | BACKGROUND COMPONENTS

The aim of this work is to estimate the total background count rate due to the space environment in the part of the orbit ideal for gamma ray transient observations, that is, outside SAA and polar regions, which contain high fluxes of geomagnetically trapped particles. Spectra of various background components are used as input in the full Monte Carlo (MC) simulation applied in Geant4[1] (Agostinelli et al. 2003; Allison et al. 2016), together with the satellite's mass model.

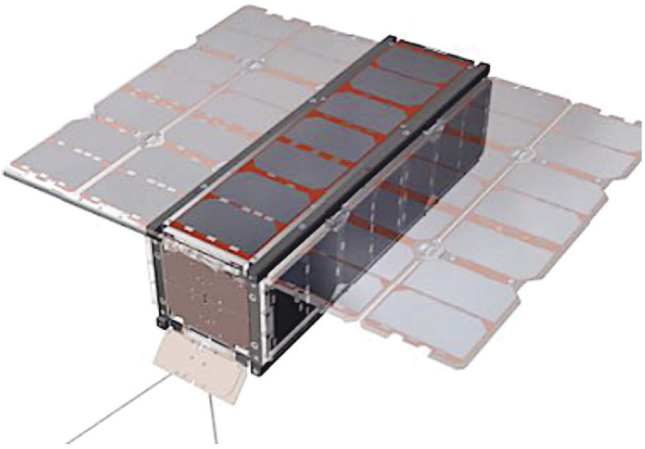

FIGURE 1 A schematic of one satellite of the *CAMELOT* constellation that can use a 3U CubeSat platform developed by C3S LLC for the RadCube mission

2.1 | Trapped particles

For the fluxes of the trapped e^- and p^+, the AE9 and AP9 models (Ginet et al. 2013) implemented in ESA's SPace ENVironment Information System (SPENVIS[2]) were used, respectively. AE9/AP9 models are based on 33 satellite datasets from 1976 to 2011 developed by U.S. Air Force Research.[3] The parameters of these models were set to MC mode with 100 runs and mean aggregate.

Averaged fluxes of e^- and p^+ over three circular orbits (avoiding crossing SAA) at an altitude of 500 km outside SAA and polar regions with inclination $i = 20°$ were simulated in SPENVIS. Figures 2 and 3 show maps of trapped e^- and p^+, respectively. The flux of trapped p^+ outside SAA is negligible. The orbit-averaged differential spectrum of trapped e^- is shown in Figure 4. The integral flux ($E > 40$ keV) is 2.0 cm^{-2} s^{-1}.

[1] https://geant4.web.cern.ch
[2] www.spenvis.oma.be
[3] https://www.vdl.afrl.af.mil/programs/ae9ap9

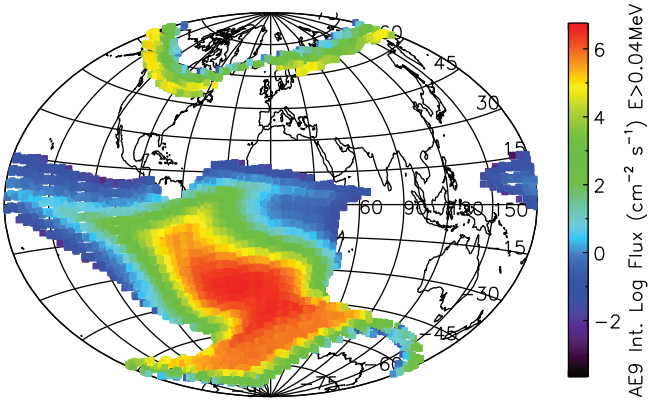

FIGURE 2 A map of the integral flux of geomagnetically trapped electrons at an altitude of 500 km according to the AE9 model (MC mode, 50% CL)

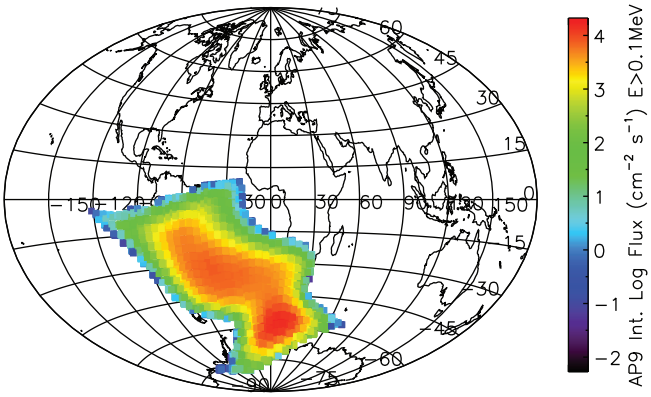

FIGURE 3 A map of the integral flux of geomagnetically trapped protons at an altitude of 500 km according to the AP9 model (MC mode, 50% CL)

2.2 | Cosmic X-ray background

The isotropic cosmic X-ray background (CXB) (see Boldt (1981); Campana et al. (2013); Fabian (1985); Giacconi et al. (1962); Mizuno et al. (2004)) can originate from the summation of the emission of extragalactic sources (active galactic nuclei, quasistellar objects, supernovae Ia, galaxy clusters, starburst galaxies, and hot intergalactic gas) (details in Ajello et al. (2008); Bagoly et al. (1988); Bi et al. (1990, 1991); Dean et al. (2003); Jahoda et al. (1991); Ma et al. (2018); Mészáros & Mészáros (1987, 1988); Shanks et al. (1991); Sreekumar et al. (1998)). Another origin discussed in literature is due to the Cosmic Microwave Background (Penzias & Wilson 1965) inverse Compton scattered on cosmic ray electrons (see Dean et al. (2003) and references therein). For our simulations, we used the model by Gruber et al. (1999), which models the low-energy and high-energy parts of the CXB measurements from *HEAO-1* (Rothschild et al. 1979), *CGRO*/COMPTEL, and *CGRO/EGRET* (Gehrels et al. 1993) instruments over the wide range of energies from 3 keV to 100 GeV. This model is used as a standard in modeling of CXB for space missions.

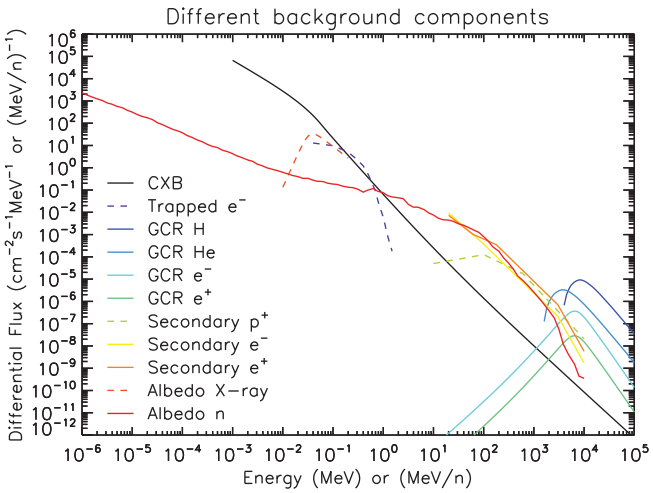

FIGURE 4 Spectra of all background components (particles and X-rays) used to irradiate the mass model of the satellite in the Geant4 simulations

The flux is omnidirectional, and at an altitude of 500 km, it irradiates the satellite from the solid angle of 8.64 srad (3.93 srad is occulted by the Earth). The CXB spectrum used for the Geant4 simulations is shown in Figure 4. The integral flux ($E > 10$ keV) is 30.3 cm^{-2} s^{-1}.

2.3 | Galactic cosmic rays

The spectra of primary particles of the galactic cosmic rays (GCR) used in the Geant4 simulations are described below and are shown in Figure 4. For an altitude of 500 km, the fluxes irradiate the satellite from the solid angle of 8.64 srad.

2.3.1 | Primary H and He

For the spectra of the primary H and He, we used the model ISO-15390,[4] implemented in SPENVIS. ISO-15390 is the international standard for estimating the radiation impact of GCR on hardware in space.

The averaged spectra were obtained for the same three orbits as described in Section 2.1 with the following parameters: solar minimum activity (May 1996), magnetic shielding on, stormy magnetosphere, Størmer with eccentric dipole method, and magnetic field moment unchanged.

The integral flux for H is 0.12 cm^{-2} s^{-1} ($E > 1$ GeV), and for He, it is 0.021 cm^{-2} s^{-1} ($E > 1$ GeV/n).

2.3.2 | Primary electrons and positrons

For the spectra of the primary e$^-$ and e$^+$, we used the model described by Mizuno et al. (2004) (see also references therein) for solar minimum (solar modulation potential $\varphi = 0.55$ GV), an altitude of 500 km, and for geomagnetic latitude $\theta_M = 20^\circ$.

[4] www.iso.org/standard/37095.html

The integral flux ($E > 1$ GeV) for e^- is 3×10^{-3} cm^{-2} s^{-1}, and for e^+, it is 2.3×10^{-4} cm^{-2} s^{-1}.

2.4 | Secondary particles and radiation

Secondary (albedo) particles and radiation originates from the interaction of GCR with the Earth's atmosphere (Jursa 1985). The fluxes used in the Geant4 simulations are described below and shown in Figure 4.

2.4.1 | Secondary protons

For the secondary p^+ and for energy above 100 MeV, we use the modeling by Mizuno et al. (2004) based on the Alpha Magnetic Spectrometer (AMS) data (Alcaraz et al. 2000a) from an altitude of 380 km for the geomagnetic latitude $17^\circ < \theta_M < 23^\circ$. For energy below 100 MeV, we use the fit to *MITA*/NINA-2 data from an altitude of 450 km (Bidoli et al. 2002) for $1.0 \leq$ L - shell ≤ 1.7. For details, see the LAT Technical Note LAT-TD-08316-01[5] of the *Fermi* satellite (Atwood et al. 2009).

There is only a small dependence of the flux on altitude (Bidoli et al. 2002; Zuccon et al. 2003); therefore, it can be used as an approximation to the flux at 500 km. The same flux model is used for upward and downward components; therefore, the flux irradiates the satellite from the solid angle of 4π srad. The integral flux ($E > 10$ MeV) is 0.037 cm^{-2} s^{-1}.

2.4.2 | Secondary electrons and positrons

For the secondary e^- and e^+ and for energy above 100 MeV, we use the modeling by Mizuno et al. (2004) based on the AMS data (Alcaraz et al. 2000b) from an altitude of 380 km for the geomagnetic latitude $0^\circ < \theta_M < 17^\circ$. For energy below 100 MeV, we use the fit to the *Mir*/MARIA-2 data from an altitude of 400 km (Voronov et al. 1991) for $1.0 \leq$ L - shell ≤ 1.2. For details, see the LAT Technical Note LAT-TD-08316-01.

The same flux model is used for upward and downward components; therefore, the flux irradiates the satellite from the solid angle of 4π srad. The integral flux ($E > 20$ MeV) is 0.18 cm^{-2} s^{-1} for e^- and 0.23 cm^{-2} s^{-1} for e^+.

2.4.3 | Albedo X-rays

The spectrum of the albedo X-rays is taken from the *Swift*/BAT measurements for an altitude of ∼550 km and inclination $i = 20.6°$ (Ajello et al. 2008). Concerning the altitude of 500 km, the flux would irradiate the satellite from the solid angle of 3.93 srad. The integral flux ($E > 10$ keV) is 2.0 cm^{-2} s^{-1}.

[5]fermi.gsfc.nasa.gov/science/resources/swg/LAT_bkgd_Rev.pdf

2.4.4 | Albedo neutrons

For the albedo neutrons, we use the predictions of the QinetiQ Atmospheric Radiation Model (QARM), based on MC radiation transport code, as reported in the ESA document ECSS-E-ST-10-04C.[6] The fluxes are scaled from 100 to 500 km as described in the document and are for the cutoff rigidity of 5 GV. The integral flux ($E > 1$ eV) is 0.61 cm^{-2} s^{-1}.

3 | SHORT GRB SPECTRUM

The main goal of the CAMELOT mission is to detect and localize short GRBs, which are associated with mergers of neutron stars and, therefore, strong sources of gravitational waves. Hence, the highest priority is to estimate the signal-to-noise ratio (SNR) expected from a typical short GRB.

The spectrum of a typical short GRB ($T_{90} < 2$ s) was constructed by considering the typical values of the spectral parameters: peak energy E_{peak}, low energy spectral slope α, and high-energy spectral slope β of the Band function (Band et al. 1993) of short GRBs detected by *Fermi*/GBM from the distributions published by Nava et al. (2011). Then, we tuned the normalization A of the spectrum to obtain the values of the integral flux in the range 10–1000 keV, equal to the median peak fluxes F (ph cm^{-2} s^{-1}) of short GRBs observed by *Fermi*/GBM in the same energy range and calculated from the Fermi GBM Burst Catalog (FERMIGBRST[7]) (see Gruber et al. (2014); Narayana Bhat et al. (2016); von Kienlin et al. (2014)).

The spectral parameters of a typical short GRB used in the Geant4 simulations are $E_{peak} = 500$ keV, $\alpha = -0.5$, and $\beta = -2.3$. The median peak flux and the spectral normalization for a time scale of 1,024 ms around a GRB peak are $F_{1024} = 2.00$ ph cm^{-2} s^{-1} and $A_{1024} = 7.8 \times 10^{-3}$ ph cm^{-2} s^{-1} keV^{-1}, respectively.

4 | MC SIMULATIONS

Full MC simulations, including the satellite's mass model in Geant4, are performed (see Figure 5). Three different thicknesses of the Al casing, 1.0, 1.5, and 2.0 mm, are considered in the simulations to check the dependence of the count rates on the material thickness.

4.1 | Description of Geant4 simulations

In order to simulate the interaction of particles, including gamma rays from GRBs and background particles, a dedicated particle physics simulation was developed using Geant4

[6]https://ecss.nl/standard/ecss-e-st-10-04c-space-environment
[7]https://heasarc.gsfc.nasa.gov/W3Browse/fermi/fermigbrst.html

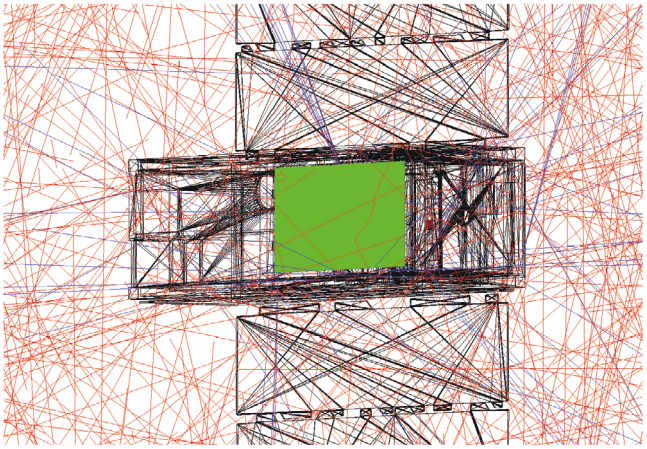

FIGURE 5 Simulation of particles and photons interacting with the mass model of the satellite in Geant4. The green rectangle marks the tracks of the optical photons produced in the scintillator of the detector

10.0.p4. In order to be as realistic as possible—to take into account the secondary particles created by the interaction of the primary particles and the material of the satellite as well—a complex computer-aided design model of the satellite was imported to the Geant4 simulation with CADMESH (Poole et al. 2012). The "Physics List" used in the simulation was chosen to be a ModularPhysicsList that included elastic hadron scattering, all relevant physics for neutrons, electromagnetic processes, and optical photon physics.

Individual (scintillation) photons with an optical wavelength were created by particles depositing energy inside the scintillator. These were tracked until they were either absorbed or detected by the SiPMs implemented in the simulation. The optical parameters of the scintillators were determined by a dedicated set of measurements. The most relevant optical parameters were attenuation length, the reflectivity of the enhanced specular reflector (ESR) tape that is planned to cover the CsI(Tl) scintillators, and the photon detection efficiency of the SiPM. The optical parameters were fine-tuned by matching the measured and simulated spectra.

4.2 | Simulation results

The detection count rates from the different components of the background obtained from the Geant4 simulations are presented in Table 1. The dominant component is CXB followed by the albedo X-rays and secondary positrons.

The Geant4 simulation for a typical short GRB with the incident flux perpendicular to the scintillator and not passing through the satellite's body gives detection count rates of 135, 130, and 125 cnt s^{-1} for Al scintillator casing thicknesses of 1.0, 1.5, and 2.0 mm, respectively. Assuming a trigger algorithm with a time window of 1 s, then SNR = GRB counts/$\sqrt{\text{background counts}}$ would be 4.3, 4.8, and 5.1 for the three Al casing thicknesses, respectively.

The detection count rates were obtained for only one CsI scintillator of size $75 \times 150 \times 5$ mm^3. Up to four CsI scintillators (two scintillators on two perpendicular sides) are planned for each CAMELOT 3U satellite.

5 | DUTY CYCLE

As seen from Figure 2, the flux of trapped e^- can increase by several orders of magnitude in the polar regions or inside SAA compared to the flux near the equator. The high increase of the background was also observed by the *Lomonosov*/BDRG (Svertilov et al. 2018), which is a gamma ray transient detector that is sensitive in the energy range from 10 keV to 3 MeV. It consists of three modules of NaI(Tl) and CsI(Tl) scintillators covered by a less than 1 mm-thick Al window shield and read out by photomultiplier tubes. The instrument shows that background count rate can increase by 50× when passing SAA or polar regions.

Therefore, we calculated the duty cycle for an altitude of 500 km and inclinations of 53° and 97.6°, which are the inclinations considered in the feasibility study of CAMELOT (Werner et al. 2018). We simulated 1,000 circular orbits at an altitude of 500 km and calculated the fraction of the time the satellite spent in the area with a high background flux of trapped e^- (>1 cm^{-2} s^{-1}). For the map of the integral fluxes of trapped e^- ($E > 40$ keV), we used the AE-8 MIN Update ESA-SEE1 model (Vampola 1998).

At an altitude of 500 km, a satellite would spend 23 and 32% of the time in the regions of flux >1 cm^{-2} s^{-1} of trapped e^- for inclinations of 53° and 97.6°, respectively.

TABLE 1 Detection background count rate (cnt s^{-1}) for one CsI(Tl) scintillator of size $75 \times 150 \times 5$ mm^3 as a function of the Al casing thickness obtained from the Geant4 simulations

			Secondary particles				GCR					
Casing (mm)	CXB	Albedo X-ray	p^+	n	e^-	e^+	H	He	e^-	e^+	Trapped e^-	Total
1.0	703	175	17	6.0	21	58	16	6.9	0.15	0.07	1.2	1,007
1.5	425	179	19	4.8	20	63	19	6.9	0.16	0.33	1.2	738
2.0	324	164	18	5.1	21	63	19	7.0	0.15	0.33	1.2	622

Abbreviations: CXB, cosmic X-ray background; GCR, galactic cosmic rays.

TABLE 2 Expected ionizing dose (rad year^{-1}) in MPPCs for an altitude of 500 km for different shielding

Shielding thickness (mm)	Trapped p^+	Solar p^+	GCR				Secondary p^+	Total
			H1	H2	He3	He4		
Inclination 53°								
No shielding	1,108	41	0.8	0.9	0.4	0.4	0.2	1,152
Al 1.0	223	1.2	0.9	1.1	0.5	0.5	0.2	227
Pb 1.0 + Al 1.0	132	0.3	1.1	1.4	0.5	0.5	0.2	136
Pb 1.5 + Al 1.0	117	0.2	1.2	1.5	0.5	0.5	0.2	121
Pb 2.0 + Al 1.0	106	0.2	1.2	1.6	0.5	0.5	0.2	110
Pb 2.5 + Al 1.0	95	0.2	1.3	1.7	0.5	0.6	0.2	99
Pb 3.0 + Al 1.0	86	0.1	1.3	1.8	0.6	0.6	0.2	90
Inclination 89.9°								
No shielding	773	1,262	1.6	1.8	0.8	0.8	0.2	2,040
Al 1.0	153	36	1.7	2.0	0.8	0.8	0.2	194
Pb 1.0 + Al 1.0	92	10	2.0	2.4	0.8	0.9	0.2	108
Pb 1.5 + Al 1.0	80	6.7	2.1	2.6	0.9	0.9	0.2	94
Pb 2.0 + Al 1.0	72	4.8	2.1	2.6	0.9	0.9	0.2	83
Pb 2.5 + Al 1.0	66	3.5	2.2	2.7	0.9	0.9	0.2	76
Pb 3.0 + Al 1.0	59	2.6	2.3	2.9	0.9	0.9	0.2	69

Abbreviations: GCR, galactic cosmic rays; MPPC, multipixel photon counters.

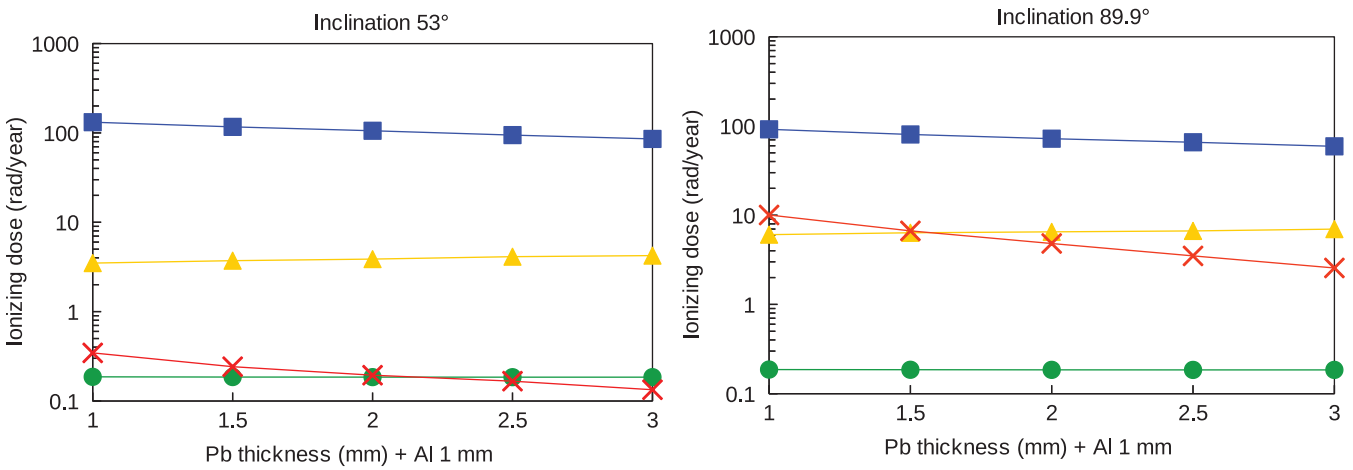

FIGURE 6 Expected annual ionizing dose in multipixel photon counters (MPPCs) due to fluxes from various sources as a function of the thickness of the lead shielding. The simulated orbits have altitude of 500 km and inclinations of 53° (left) and 89.9° (right). The sources are: trapped p^+ (blue squares), GCR H1 + H2 + He3 + He4 (yellow triangles), solar p^+ (red crosses), and secondary p^+ (green circles)

6 | EXPECTED IONIZING DOSE IN MPPC

Hamamatsu S14160-6050HS MPPCs were considered for the detectors for CAMELOT. The proton beam irradiation tests at W-MAST (Wakasa-wan, Japan) facility performed by the CAMELOT team demonstrate that the MPPCs degrade when irradiated by 200 MeV p^+. Therefore, it is necessary to estimate the expected total ionizing dose at (LEO) and to design a protective cover shielding MPPCs to decrease the total dose due to p^+.

We used Multi-Layered Shielding Simulation (MULASSIS) (Lei et al. 2002) implemented in SPENVIS to calculate ionization dose in a Si sphere shielded by Al and Pb. A simple spherical geometry with source flux isotropically incident over 4π srad was used for approximation.

The following proton sources are used in the simulation: trapped p^+ AP9 model (MC mode, 50% CL, 100 runs,

30 days of orbit simulation with 60 s sampling); solar p^+ ESP-PSYCHIC (Xapsos et al. 2007) model implemented in SPENVIS (50% CL, magnetic shielding on, stormy magnetosphere, Størmer with eccentric dipole method, magnetic field moment unchanged); and GCR p^+ ISO 15390 model (same parameter setting as described in Section 2.3.1); for secondary p^+, we use the same model as described in Section 2.4.1.

The expected annual doses for inclinations of 53° and 89.9° are shown in Table 2 and Figure 6. The irradiation tests at the W-MAST facility suggest that the considered MPPCs can be used for the CAMELOT mission when proper shielding is applied. For a 1U CubeSat demonstration mission GRBAlpha, we consider using 2.5 mm of Pb + 1.0 mm of Al.

7 | CONCLUSIONS

We studied the expected background for the CAMELOT mission and the detectability of short GRBs. It was shown that, with at least one large scintillator, short GRBs with a typical peak flux can be detected. Future work will include, for example, a study of the background activation due to the radioactive decay of elements of the detector and the satellite's body generated when passing SAA. Other transients, beside the short GRBs, such as long GRBs, SGRs, and TGFs, should also be considered. The expected annual doses allow use of the planned MPPCs for the CAMELOT mission when proper shielding against protons is applied.

ACKNOWLEDGMENTS

This research has been supported by the grants awarded by the Hungarian Academy of Sciences, Lendület LP2016-11, KEP-7/2018, and by the European Union, cofinanced by the European Social Fund (Research and development activities at the Eötvös Loránd University's Campus in Szombathely), EFOP-3.6.1-16-2016-00023.

CONFLICT OF INTERESTS

The authors declare no potential conflict of interests.

REFERENCES

Abbott, B. P., Abbott, R., Abbott, T. D., et al. 2017, *Phys. Rev. Lett.*, *119*(16), 161101.

Agostinelli, S., Allison, J., Amako, K., et al. 2003, *Nucl. Instrum. Methods Phys. Res. A*, *506*(3), 250. https://doi.org/10.1016/S0168-9002(03)01368-8.

Ajello, M., Greiner, J., Sato, G., et al. 2008, *ApJ*, *689*(2), 666.

Alcaraz, J., Alvisi, D., Alpat, B., et al. 2000a, *Phys. Lett. B*, *472*(1–2), 215.

Alcaraz, J., Alpat, B., Ambrosi, G., et al. 2000b, *Phys. Lett. B*, *484*(1–2), 10.

Allison, J., Amako, K., Apostolakis, J., et al. 2016, *Nucl. Instrum. Methods Phys. Res. A*, *835*, 186.

Atwood, W. B., Abdo, A. A., Ackermann, M., et al. 2009, *ApJ*, *697*(2), 1071.

Bagoly, Z., Mészáros, A., & Mészáros, P. 1988, *ApJ*, *333*, 54.

Band, D., Matteson, J., Ford, L., et al. 1993, *ApJ*, *413*, 281.

Bi, H., Mészáros, A., & Mészáros, P. 1990, in: The Galactic and Extragalactic Background Radiation, S. Bowyer & C. Leinert (Eds.), IAU Symposium, Vol. 139, 416.

Bi, H., Mészáros, A., & Mészáros, P. 1991, *A&A*, *243*(1), 16.

Bidoli, V., Casolino, M., de Pascale, M., et al. 2002, *Ann. Geophys.*, *20*(10), 1693.

Boldt, E. 1981, *Comments Astrophys.*, *9*, 97.

Campana, R., Feroci, M., Del Monte, E., Mineo, T., Lund, N., & Fraser, G. W. 2013, 36, *Exp. Astron.*, *3*, 451.

Dean, A. J., Bird, A. J., Diallo, N., et al. 2003, *Space Sci. Rev.*, *105*, 285.

Fabian, A. C. 1985, in: *Observational and Theoretical Aspects of Relativistic Astrophysics and Cosmology*, eds. L.-J. Goicoechea & J.-L. Sanz, 103, World Scientific (Singapore).

Fishman, G. J., Bhat, P. N., Mallozzi, R., et al. 1994, *Science*, *264*(5163), 1313.

Gehrels, N., Chipman, E., & Kniffen, D. A. 1993, *A&AS*, *97*, 5.

Giacconi, R., Gursky, H., Paolini, F. R., & Rossi, B. B. 1962, *Phys. Rev. Lett.*, *9*(11), 439.

Ginet, G. P., O'Brien, T. P., Huston, S. L., et al. 2013, *Space Sci. Rev.*, *179*, 579.

Goldstein, A., Veres, P., Burns, E., et al. 2017, *ApJ*, *848*(2), L14.

Gruber, D. E., Matteson, J. L., Peterson, L. E., & Jung, G. V. 1999, *ApJ*, *520*(1), 124.

Gruber, D., Goldstein, A., Weller von Ahlefeld, V., et al. 2014, *ApJS*, *211*(1), 12.

Jahoda, K., Lahav, O., Mushotzky, R. F., & Boldt, E. 1991, *ApJ*, *378*, L37.

Jursa, A. S. 1985, *Handbook of Geophysics and the Space Environment*, Air Force Geophysics Laboratory (Springfield).

von Kienlin, A., Meegan, C. A., Paciesas, W. S., et al. 2014, *ApJS*, *211*(1), 13.

Klebesadel, R. W., Strong, I. B., & Olson, R. A. 1973, *ApJ*, *182*, L85.

Kouveliotou, C., Dieters, S., Strohmayer, T., et al. 1998, *Nature*, *393*, 235.

Kouveliotou, C., Wijers, R. A. M. J., & Woosley, S. 2012, *Gamma-Ray Bursts*, Cambridge University Press (Cambridge).

Lei, F., Truscott, P. R., Dyer, C. S., et al. 2002, *IEEE Trans. Nucl. Sci.*, *49*(6), 2788.

Ma, Q., Ciardi, B., Eide, M. B., & Helgason, K. 2018, *MNRAS*, *480*(1), 26.

Mazets, E. P., Golentskii, S. V., Ilinskii, V. N., Aptekar, R. L., & Guryan, I. A. 1979, *Nature*, *282*, 587.

Mészáros, A., & Mészáros, P. 1987, *Publ. Astron. Inst. Czech. Acad. Sci.*, *4*, 445.

Mészáros, A., & Mészáros, P. 1988, *ApJ*, *327*, 25.

Mizuno, T., Kamae, T., Godfrey, G., et al. 2004, *ApJ*, *614*(2), 1113.

Narayana Bhat, P., Meegan, C. A., von Kienlin, A., et al. 2016, *ApJS*, *223*(2), 28.

Nava, L., Ghirlanda, G., Ghisellini, G., & Celotti, A. 2011, *A&A*, *530*, A21.

Ohno, M., Werner, N., Pál, A. et al. 2018, in: CAMELOT: Design and Performance Verification of the Detector Concept and Localization Capability, eds. J.-W. A. den Herder, S. Nikzad, & K. Nakazawa, Proc. SPIE, Vol. 10699, 1069964.

Pál, A., Mészáros, L., Tarcai, N. et al. 2018, CAMELOT—Concept study and early results for onboard data processing and GPS-based timestamping. arXiv:1806.03685.

Penzias, A. A., & Wilson, R. W. 1965, *ApJ*, *142*, 419.

Poole, C. M., Cornelius, I., Trapp, J. V., & Langton, C. M. 2012, *Australas. Phys. Eng. Sci. Med.*, *35*, 329.

Řípa, J., Werner, N., Ohno, M. et al. 2018, 69th International Astronautical Congress, IAC-18,B4,2,8,x46335.

Rothschild, R., Boldt, E., Holt, S., et al. 1979, *Space Sci. Instrum.*, *4*, 269.

Shanks, T., Georgantopoulos, I., Stewart, G. C., Pounds, K. A., Boyle, B. J., & Griffiths, R. E. 1991, *Nature*, *353*(6342), 315.

Sreekumar, P., Bertsch, D. L., Dingus, B. L., et al. 1998, *ApJ*, *494*, 523.

Svertilov, S. I., Panasyuk, M. I., Bogomolov, V. V., et al. 2018, *Space Sci. Rev.*, *214*(1), 8.

Torigoe, K., Fukazawa, Y., Galgóczi, G., et al. 2019, *Nucl. Instrum. Methods Phys. Res. A*, *924*, 316.

Vampola, A. L. 1998, Conf. High Energy Radiat. Background Space. Workshop Record, IEEE, 128.

Vedrenne, G., & Atteia, J.-L. 2009, Gamma-Ray Bursts: The brightest explosions in the Universe. Berlin: Springer.

Voronov, S. A., Gal'Per, A. M., Koldashov, S. V., Maslennikov, L. V., Mikhailov, V. V., & Popov, A. V. 1991, *Kosmicheskie Issledovaniia*, *29*, 567.

Werner, N., Řípa, J., Pál, A. et al. 2018, in: CAMELOT: Cubesats Applied for MEasuring and LOcalising Transients Mission Overview, eds. J.-W. A. den Herder, S. Nikzad, & K. Nakazawa, Proceedings of the SPIE, Vol. 10699, 106992P.

Xapsos, M. A., Stauffer, C., Jordan, T., Barth, J. L., & Mewaldt, R. A. 2007, *IEEE Trans. Nucl. Sci.*, *54*(6), 1985.

Zuccon, P., Bertucci, B., Alpat, B., et al. 2003, *ICRC*, *7*, 4249.

AUTHOR BIOGRAPHY

Jakub Řípa received the Master's degree in physics in 2006 and the PhD degree in astronomy and astrophysics in 2011, both at the Charles University (MFF UK), Prague, Czech Republic under the supervision of doc. RNDr. Attila Mészáros, DrSc. He was a postdoctoral researcher at Institute for the Early Universe, Ewha Womans University, Seoul, Korea (2011–2012); Institute of Basic Science, Sungkyunkwan University, Suwon, Korea (2012–2015); Leung Center for Cosmology and Particle Astrophysics, National Taiwan University, Taipei, Taiwan (2015–2017). Currently, he is a postdoctoral researcher at the Astronomical Institute, Charles University and at the Lendület Hot Universe Research Group, MTA-Eötvös University, Budapest, Hungary. His research interests include gamma-ray bursts and instrumentation for high-energy astrophysics in hard X-rays and gamma-rays.

How to cite this article: Řípa J, Galgóczi G, Werner Norbert, Pál András, Ohno Masanori, Mészáros László, Mizuno Tsunefumi, Tarcai Norbert, Torigoe K, Uchida N, Fukazawa Yasushi, Takahashi H, Nakazawa Kazuhiro, Hirade Naoyoshi, Hirose Kengo, Hisadomi Syohei, Enoto T, Odaka Hirokazu, Ichinohe Yuto, Frei Z, Kiss László. Estimation of the detected background by the future gamma ray transient mission CAMELOT. *Astron. Nachr*. 2019;340:666–673. https://doi.org/10.1002/asna.201913673